# The Offner imaging spectrometer in quadrature

**Xesús Prieto-Blanco, Carlos Montero-Orille, Héctor González-Nuñez, María Dolores Mouriz, Elena López Lago, and Raúl de la Fuente***

*Departamento de Física Aplicada, Escola Universitaria de Óptica e Optometría, Universidade de Santiago de Compostela, 15782 Galicia, Spain*
**raul.delafuente@usc.es*

**Abstract:** This is a proposal and description of a new configuration for an Offner imaging spectrometer based on the theory of aberrations of off-plane classical-ruled spherical diffraction gratings. This new spectrometer comprises a concave mirror used in double reflection and a convex reflection grating operating in quadrature, in a concentric layout. A very simple procedure obtains designs that are anastigmatic for a given point on the entrance slit and a given wavelength. Specific examples show that the performance of this type of system improves the performance of analogous conventional in-plane systems, when compactness and/or high spectral resolution is of fundamental importance.



**OCIS codes:** (120.6200) Spectrometers and spectroscopic instrumentation; (220.2740) Geometric optical design; (220.4830) Systems design.

## References and links

1. D. R. Lobb, "Imaging spectrometer using concentric optics," Proc. SPIE **3118**, 339–347 (1997).
2. P. Mouroulis, R. O. Green, and D. W. Wilson, "Optical design of a coastal ocean imaging spectrometer," Opt. Express **16**(12), 9087–9096 (2008).
3. D. W. Warren, D. J. Gutierrez, and E. R. Keim, "Dyson spectrometers for high performance infrared applications," Opt. Eng. **47**(10), 103061 (2008).
4. N. C. Das, and M. V. R. K. Murty, ""Flat field spectrograph using convex holographic diffraction grating and concave mirror," Pramäna-," J. Phys. **27**, 171–192 (1986).
5. D. Kwo, G. Lawrence, and M. Chrisp, "Design of a grating spectrometer from a 1:1 Offner mirror system," Proc. SPIE **818**, 275–279 (1987).
6. M. P. Chrisp, "Convex diffraction grating imaging spectrometer," U.S. Patent nº 5,880,834 (1999).
7. P. Mouroulis, and M. M. McKerns, "Pushbroom imaging spectrometer with high spectroscopy data fidelity: experimental demonstration," Opt. Eng. **39**(3), 808–816 (2000).
8. C. Davis, J. Bowles, R. Leathers, D. Korwan, T. V. Downes, W. Snyder, W. Rhea, W. Chen, J. Fisher, P. Bissett, and R. A. Reisse, "Ocean PHILLS hyperspectral imager: design, characterization, and calibration," Opt. Express **10**(4), 210–221 (2002).
9. X. Prieto-Blanco, C. Montero-Orille, B. Couce, and R. de la Fuente, "Analytical design of an Offner imaging spectrometer," Opt. Express **14**(20), 9156–9168 (2006).
10. P. Mouroulis, "Low-distortion imaging spectrometer design utilizing convex gratings," Proc. SPIE **3482**, 594–601 (1998).
11. C. Whyte, R. J. Leigh, D. Lobb, T. Williams, J. J. Remedios, M. Cutter, and P. S. Monks, "Assessment of the performance of a compact concentric spectrometer system for Atmospheric Differential Optical absorption Spectroscopy," Atmos. Meas. Tech. **2**(2), 789–800 (2009).
12. S. Kayser, B. Sang, J. Schubert, S. Hofer, and T. Stuffler, "Compact prism spectrometer of pushbroom type for Hyperspectral imaging," Proc. SPIE **7100**, 710014 (2008).
13. F. M. Reininger, "Imaging spectrometer/camera having convex grating," U.S. Patent nº 6,100,974 (2000).
14. R. L. Lucke, "Out-of-plane dispersion in an Offner spectrometer," Opt. Eng. **46**(7), 073004 (2007).
15. X. Prieto-Blanco, C. Montero-Orille, H. González-Núñez, M. D. Mouriz, E. López Lago, and R. de la Fuente, "Imaging with classical spherical diffraction gratings: the quadrature configuration," J. Opt. Soc. Am. A **26**(11), 2400–2409 (2009).
16. OSLO is a registered trademark of Lambda Research Corporation, 80 Taylor Street, P.O. Box 1400, Littleton, Mass. 01460.

#126592 - $15.00 USD Received 6 Apr 2010; revised 14 May 2010; accepted 14 May 2010; published 28 May 2010

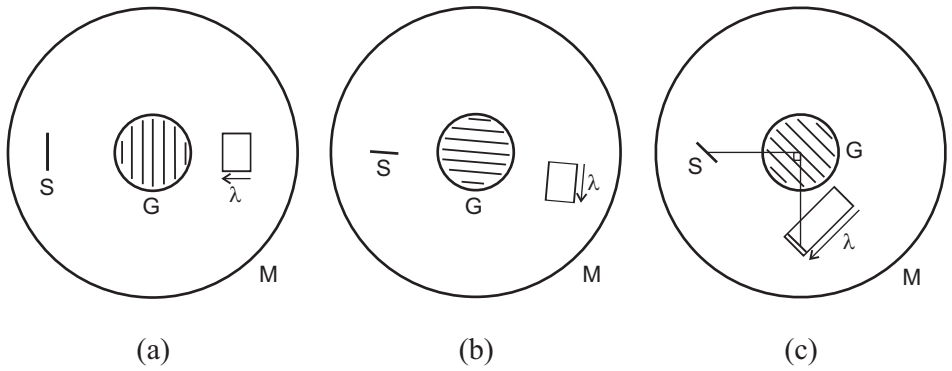


Fig. 1. View along the optical axis of three different configurations of the Offner imaging spectrometer. Each plot shows the diffraction grating (G), the concave mirror (M), the slit (S) and its spectral images. (a) The in-plane configuration. (b) The off-plane configuration included in [13,14]. This configuration can be obtained by rotating in configuration (a) the slit and grating grooves at an angle close to 90°. (c) The quadrature configuration. It can be obtained by rotating in configuration (a) the slit and grating grooves at an angle of 45°.

## 1. Introduction

Imaging spectrometers that use spherical and concentric optics have been proved highly attractive as they allow for a simple set-up and a very compact configuration with high optical performance over the whole spectral range of the system. Various concentric designs can be distinguished, such as the Dyson type [1–3], the Offner type [4–9] or the near-Littrow mounting [10,11]. Among these, the Offner spectrometer has received the most analysis. It has been shown to provide a high signal to noise ratio and small spot sizes together with low spatial and spectral distortions [7–9]. This spectrometer is based on the Offner imaging system comprising a concave primary and tertiary mirror and a convex secondary mirror. In the spectrometer design, the secondary mirror is replaced by a reflective convex diffraction grating [4,5] (other proposed systems use curved prisms as the dispersive elements [10,12]). Since diffraction at the grating lacks the symmetry of specular reflection, a further improvement is achieved by splitting the concave mirror into two concentric mirrors of different radii [7–9].

Figure 1a shows a view along the optical axis of a typical Offner spectrometer. For simplicity, a two reflector system has been drawn with a single concave mirror used in double reflection. The entrance slit and the two-dimensional spectral image are arranged on opposite sides of the diffraction grating in a direction perpendicular to the slit itself. This is the in-plane configuration, which is used in almost all imaging spectrometers. In the literature, there are many examples of in-plane Offner spectrometer designs with two and three reflectors [4–9]; an analytical approach to the design of such spectrometers with small astigmatism is presented in particular in [9]. Figure 1b shows an unusual arrangement in which the slit and the spectral images are laid out in a direction essentially perpendicular to that of Fig. 1a. This is the off-plane configuration considered in refs [13,14]. Based on a heuristic assumption, Lucke [14] showed by means of examples that this configuration may be of interest if the spectrometer entrance slit is short enough.

Figure 1c plots a different off-plane arrangement. In this configuration, the slit and the spectral images are significantly displaced to one side of the spectrometer. This is the configuration studied in this work. Specific attention is given to configurations in which one point on the slit and its image for a chosen wavelength are located on lines that intersect at right angles at the center of curvature of the reflectors. The design is based on results obtained in a previous work [15]. In that work, we reviewed the theory of classical spherical diffraction gratings in off-plane arrangements. The study focused on the quadrature configuration where the incident and diffraction planes are orthogonal to each other. The main results of that work that are relevant to this paper are summarized in section two. Section three applies these

#126592 - $15.00 USD Received 6 Apr 2010; revised 14 May 2010; accepted 14 May 2010; published 28 May 2010

results to the design of an Offner imaging spectrometer in the quadrature configuration. Section four gives specific examples of such a design. Finally, a summary and conclusions are given in section 5.

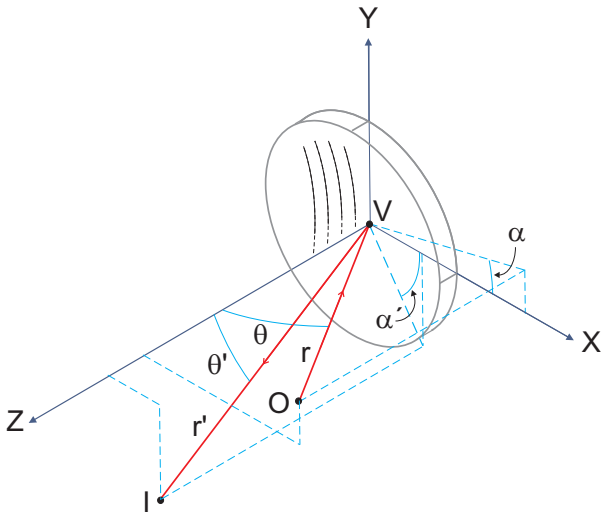


Fig. 2. Scheme of the spherical diffraction grating. The diffraction grating surface is tangent to the XY plane at its vertex $V$. Light from the object point $O$ is diffracted towards point $I$. The ray following the path $OVI$ is the reference ray. The plane of incidence is defined as the plane containing the Z axis and the ray $OV$. It makes an angle $\alpha$ with the XZ plane. The plane of diffraction is defined as the plane containing the Z axis and the ray $VI$. It makes an angle $\alpha'$ with the XZ plane.

## 2. Classical spherical gratings in the quadrature configuration

Figure 2 shows a schematic view of a classical spherical grating and presents the notation used in the text. To make the plotting clear, we have drawn a concave diffraction grating but all the results in this section apply to convex gratings as well. The main difference with regard to the drawing lies in that a convex grating provides a virtual image of a real object. The origin of the coordinates is placed at the grating vertex ($V$) and the Z axis is perpendicular to the grating at this point. The projections of the grating grooves on a plane tangent to vertex $V$ are straight lines parallel to the Y axis with regular spacing $d$. The plot also shows a point source $O$ located at an arbitrary position specified by the spherical coordinates $(r,\theta,\alpha)$ and its image for a given diffraction order $m$, $I(r',\theta',\alpha')$. The angle $\theta(\theta')$ corresponds to the angle of incidence (diffraction) of the reference ray $OV$ ($VI$) in the diffraction grating, whereas angle $\alpha(\alpha')$ is the angle that the incidence (diffraction) plane makes with the XZ plane. As usual, the incidence plane is defined as the plane that contains the incident reference ray and the Z axis; the diffraction plane is defined in a similar way. The in-plane configuration corresponds to $\alpha = 0$ and in this case $\alpha'$ is also zero. Otherwise, the configuration is off-plane. The angular coordinates of the source and image points at a wavelength $\lambda$ are related through the generalized Bragg equations. By using our notation, they read:

$$\sin\theta\cos\alpha + \sin\theta'\cos\alpha' = m\frac{\lambda}{d} \tag{1a}$$

$$\sin\theta\sin\alpha + \sin\theta'\sin\alpha' = 0 \tag{1b}$$

#126592 - $15.00 USD Received 6 Apr 2010; revised 14 May 2010; accepted 14 May 2010; published 28 May 2010

By using the aberration theory, it is not difficult to show that the grating exhibits astigmatism, so point I is really the center of one of the two astigmatic line images of O. Distance ( $r'$ ) from the origin of coordinates to point I corresponds to one of the two possible solutions of the following equation [15]:

$$\left(\frac{1+\cos^2\theta}{r}+\frac{1+\cos^2\theta'}{r'}-2\frac{\cos\theta+\cos\theta'}{R}\right)^2 = \left(\frac{\sin^2\theta}{r}-\frac{\sin^2\theta'}{r'}\right)^2+4\frac{\sin^2\theta\sin^2\theta'}{rr'}\cos^2\left(\alpha'-\alpha\right) \tag{2}$$

where $R$ is the grating radius.

This equation can be split into two simple equations when $\alpha'=\alpha$ or $\alpha'=\alpha\pm\pi/2$. The first relationship $\alpha'=\alpha$ is satisfied in specular reflection ( $m=0$ and $\theta'=-\theta$ ). It is also satisfied in the in-plane configuration where both $\alpha$ and $\alpha'$ are zero. In those cases, Eq. (2) splits into the Coddington equations for gratings and mirrors:

$$\frac{\cos^2\theta}{r}+\frac{\cos^2\theta'}{r'}=\frac{\cos\theta+\cos\theta'}{R}, \tag{3a}$$

$$\frac{1}{r}+\frac{1}{r'}=\frac{\cos\theta+\cos\theta'}{R} \tag{3b}$$

Equation (3a) corresponds to the meridional image, that is, the image set up by a bundle of rays propagating into the plane of incidence, while Eq. (3b) corresponds to the sagittal image which is set up by rays that intersect the grating in a plane orthogonal to the incident one. In the case of mirrors or $m=0$, Eq. (3b) has a simple geometrical interpretation: the object, the reflector's curvature center and the sagittal image are on the same line.

When they are used in an in-plane configuration, some concave grating monochromators make use of the Rowland design, where the center of the entrance slit is set on the Rowland circle (a circle of diameter R tangent to the grating vertex). In such a case, the meridional image is free of coma and located in the same circle, regardless of wavelength. With Eq. (3a), the Rowland condition means that if $r=R\cos\theta$, then $r'=R\cos\theta'$. It is worthwhile to note that the same condition applies for specular reflection with $\theta'=-\theta$.

The second relationship $\alpha'-\alpha=\pm\pi/2$ (hereafter, the quadrature condition) leads to the quadrature configuration in which the plane of incidence and the plane of diffraction are orthogonal to each other. In this case, Eq. (2) splits into

$$\frac{\cos^2\theta}{r}+\frac{1}{r'}=\frac{\cos\theta+\cos\theta'}{R} \tag{4a}$$

$$\frac{1}{r}+\frac{\cos^2\theta'}{r'}=\frac{\cos\theta+\cos\theta'}{R} \tag{4b}$$

Moreover, taking into account the quadrature condition, we obtain from Eq. (1b):

$$\sin\theta'=\sin\theta\tan\left|\alpha\right| \tag{5}$$

and by using Eq. (1a):

$$\sin\theta=m\frac{\lambda}{d}\cos\alpha \tag{6}$$

Equation (6) gives the wavelength that diffracts 'in quadrature' as a function of the angular coordinates of the object point, the groove spacing and the diffraction order. Equations (4) and

#126592 - $15.00 USD Received 6 Apr 2010; revised 14 May 2010; accepted 14 May 2010; published 28 May 2010

(5) give the coordinates of the center of the two astigmatic line images corresponding to a specific object position. Some simple solutions of these equations are analyzed in ref [15]. For example, when $r' = r\tan^2\alpha$, the two solutions of Eq. (4)a) and Eq. (4b) match up, and the image is anastigmatic. However, for this work, two other solutions are of special interest:

i) When the object is at $r^a = R\cos\theta$ its astigmatic line image corresponding to the solution of Eq. (4a) is at $r'^a = R/\cos\theta'$. It is important to note that this image is set up by rays that intersect the grating along the plane of incidence, as shown in Fig. 3a. Also, this set of rays does not present coma [15].

ii) When the object is at $r^b = R/\cos\theta$ its astigmatic line image corresponding to the solution of Eq. (4b) is at $r'^b = R\cos\theta'$. This image is set up by rays that intersect the grating on the plane of diffraction (see Fig. 3b). Neither do these rays exhibit coma.

These two solutions exhibit an interesting property, which is shown in Fig. 3: they can be inferred one from the other by reversing the direction of energy flow. This property is essential for the design of the Offner spectrometers proposed in this work.

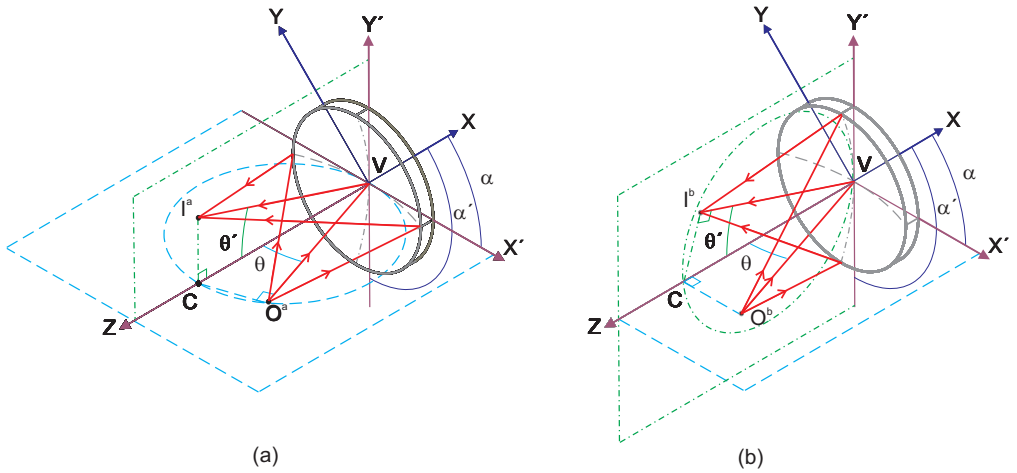


Fig. 3. Ray tracing in the quadrature configuration. Note that this figure is rotated with respect to Fig. 2. The projections of grating grooves on the XY plane are parallel to the Y axis. The X'Z plane is the plane of incidence and the Y'Z plane is the plane of diffraction. (a) The object distance from the grating vertex $V$ is $r^a = R\cos\theta$. Rays are shown converging on the image located at a distance $r'^a = R/\cos\theta'$ from the vertex. (b) The object distance from the grating vertex $V$ is $r^b = R/\cos\theta$. Rays are shown converging on the image located at a distance $r'^b = R\cos\theta'$ from the vertex.

#126592 - $15.00 USD Received 6 Apr 2010; revised 14 May 2010; accepted 14 May 2010; published 28 May 2010

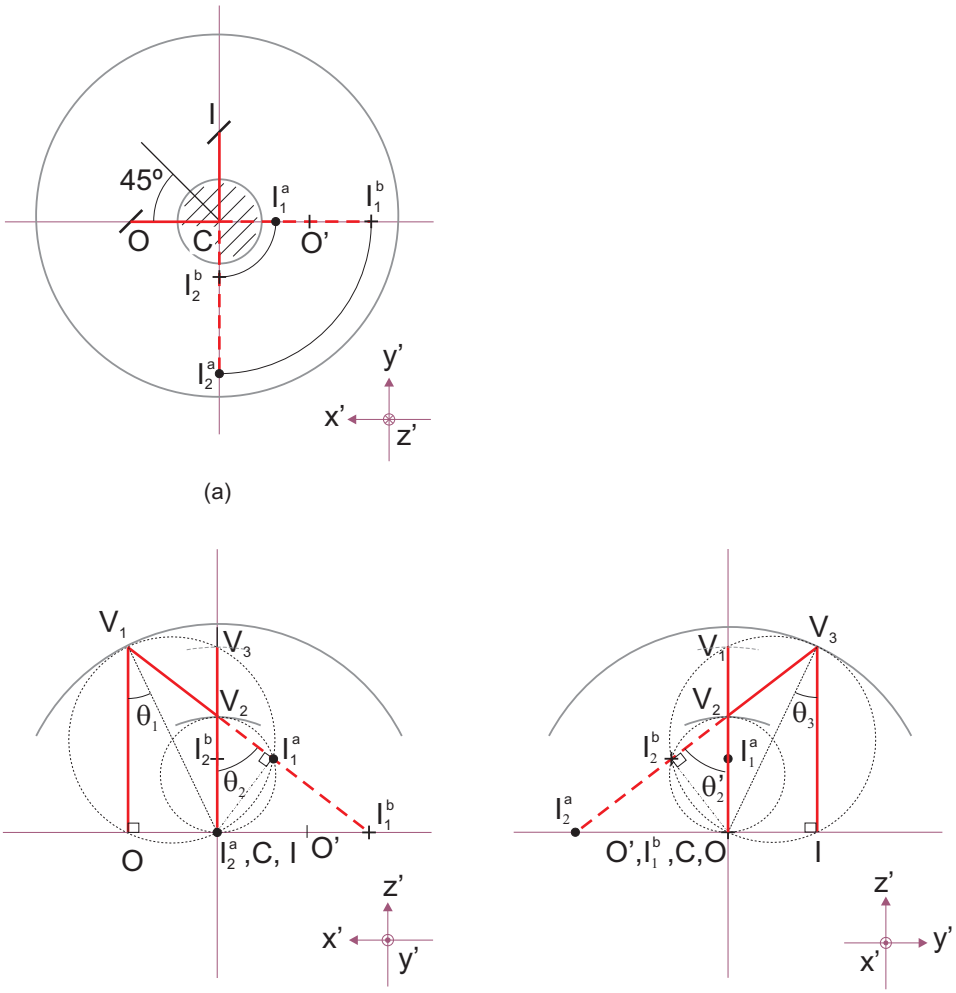


Fig. 4. Three different views of an Offner spectrometer in quadrature. (a) front view; (b) top view; (c) side view. $C$ is the common center of curvature of the convex diffraction grating and concave mirror. $O$ is the design point, $O'$ is its specular image and $I$ the spectral image at order m for the design wavelength $\lambda$ . $V_1$, $V_2$, $V_3$ are the vertices, i.e., the points of incidence of the reference ray on the reflectors. $I_1^a$, $I_1^b$, $I_2^a$ and $I_2^b$ are intermediate images.

### 3. Offner spectrometer in quadrature

We have designed an Offner type concentric spectrometer by applying the results of section 2. The main characteristic of this design is that image $I$ of a given object point $O$ on the entrance slit is anastigmatic for the wavelength $\lambda_q$ that diffracts in quadrature. Hereafter, we refer to $O$ and $\lambda_q$ as the design point and the design wavelength, respectively. In Fig. 4 we plot three different views of such a spectrometer showing its main features. To obtain clear drawings, we have taken the reference system X'Y'Z' with axis parallel to $OC$, $CI$ and $CV_2$, where $C$ is the center of curvature and $V_2$ the grating vertex. Both slit and grating grooves

#126592 - $15.00 USD Received 6 Apr 2010; revised 14 May 2010; accepted 14 May 2010; published 28 May 2010

are oriented at 45° in respect of this reference system. This means that $\alpha = \pi/4$ and, from Eq. (5), that the angle of diffraction matches the angle of incidence on the grating [ $\theta_2' = \theta_2$ in Figs. 4(b) and 4(c)]. In this symmetric case, anastigmatism can be achieved with only one concave mirror in a double reflection pass, as with an Offner imaging system. This simplifies the set-up. In the plot, we trace the path of the reference ray. This ray goes through the center of the grating surface which is the aperture stop. We also show the location of the intermediate images and the specular or zero order image ( $O'$ ).

The following explains why the above design is anastigmatic for object point $O$ and wavelength $\lambda_q$. The fundamental idea is to get astigmatic images ( $I_1^a$ and $I_1^b$ ) from the concave mirror located at distances $r^a$, $r^b$ from the grating vertex ( $V_2$ ) noted in points i) and ii) of the previous section. That is, at distances from $V_2$ $r^a = R_2 \cos\theta_2$ and $r^b = R_2/\cos\theta_2$, respectively, where $R_2$ is the grating radius. Considering the design wavelength, the grating re-images these images on an orthogonal plane, crossing their positions. That means that image $I_2^a$ is at $r'^a = R_2/\cos\theta_2$ from $V_2$ and image $I_2^b$ at $r'^b = R_2 \cos\theta_2$, both on the Y'Z' plane. Therefore, these two sets of images are arranged symmetrically from the optical axis Z', but in perpendicular planes. It follows that the second reflection in the concave mirror is mimetic with respect to the first one, and therefore the two final images meet at the same point $I$ (exactly as there is one object point for the two intermediate images $I_1^a$ and $I_1^b$). Furthermore, distance $IV_3$ is the same as $OV_1$.

Let us now determine the object position that makes $O$ image into $I_1^a$ and $I_1^b$. To obtain the position of $O$, first observe that $I_1^a$ is at the Rowland circle associated with the first reflection on the concave mirror and $I_1^b$ is on the X' axis. Taking into account the discussion on Eq. (3), it follows that the object is also located on the X' axis at a distance $r = R_1 \sin\theta_1$ from C. This is the position illustrated in Fig. 4.

The next step consists in determining the ratio of the radii. The geometry in Figs. 4b and 4c shows that $\theta_2 = 2\theta_1 = 2\theta_3$. Moreover, the concentricity implies that $R_1 \sin\theta_1 = R_2 \sin\theta_2$. These two conditions determine the radii ratio as $R_1/R_2 = 2\cos\theta_1$. Note that this relation also holds for the Offner spectrometer in the in-plane configuration [6,9].

In order to understand this better, two bundles of rays are tracked separately in Figs. (5) and (6): rays that depart from $O$ along the X'Z' plane (Fig. 5) and rays that depart from $O$ along a plane parallel to the Y'Z' plane (Fig. 6). The first form an image (the meridional image) of $O$ at point $I_1^a$ upon a first reflection on the concave mirror (Figs. 5a and 5b). Now taking $I_1^a$ as a virtual object point with respect to the diffraction grating, it is imaged on $I_2^a$ at the Y' axis below $C$ (Figs. 5c and 5d). Finally, the concave mirror images $I_2^a$ into the final (sagittal) image I at the Y' axis too, but above $C$ (Figs. 5e and 5f). The second set of rays is tracked in a similar way. They follow the paths depicted in Fig. 6. They are sagittal rays upon the first reflection in the concave mirror and they are meridional rays in the second reflection in this mirror. The intermediate images are located at points $I_1^b$ and $I_2^b$ and the final image matches the one obtained by the previous bundle of rays. Note the symmetry between these two bundles of rays: ray tracing in Fig. 6 can be obtained from Fig. 5 by reversing the path direction, which means taking $I$ as the object point and $O$ the final image. This symmetry results from the fact that meridional rays incident on the grating become sagittal rays when emerging from the grating, and vice versa.

#126592 - $15.00 USD Received 6 Apr 2010; revised 14 May 2010; accepted 14 May 2010; published 28 May 2010

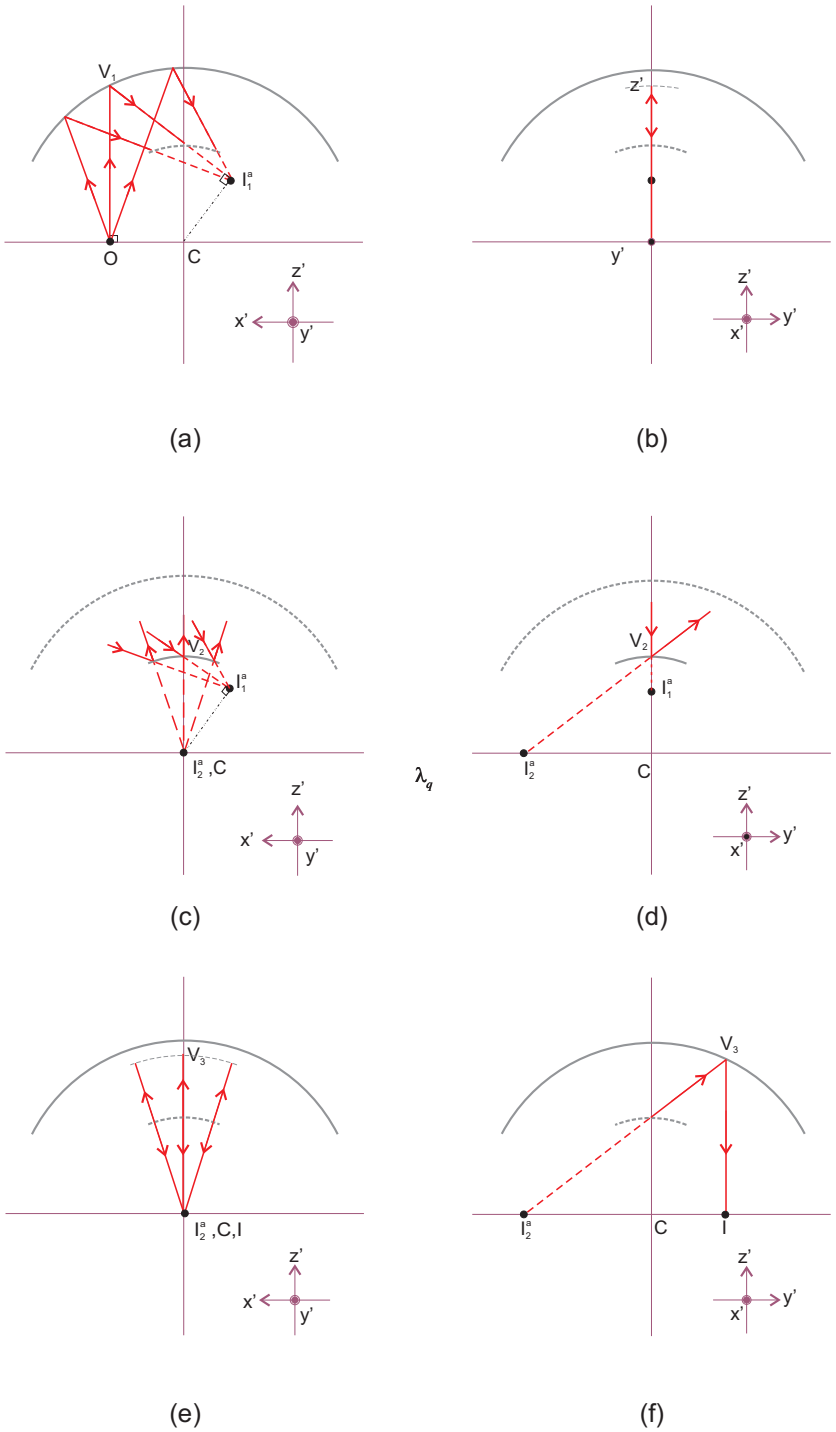


Fig. 5. Top view (a)-(c)-(e) and side view (b)-(d)-(f) of the Offner spectrometer in quadrature showing the path followed by the bundle of rays that depart from the design point $O$ in the X'Z' plane. (a) and (b) show the first reflection on the concave mirror; (c) and (d) show the reflection on the diffraction grating; (e) and (f) show the second reflection on the concave mirror.

#126592 - $15.00 USD Received 6 Apr 2010; revised 14 May 2010; accepted 14 May 2010; published 28 May 2010

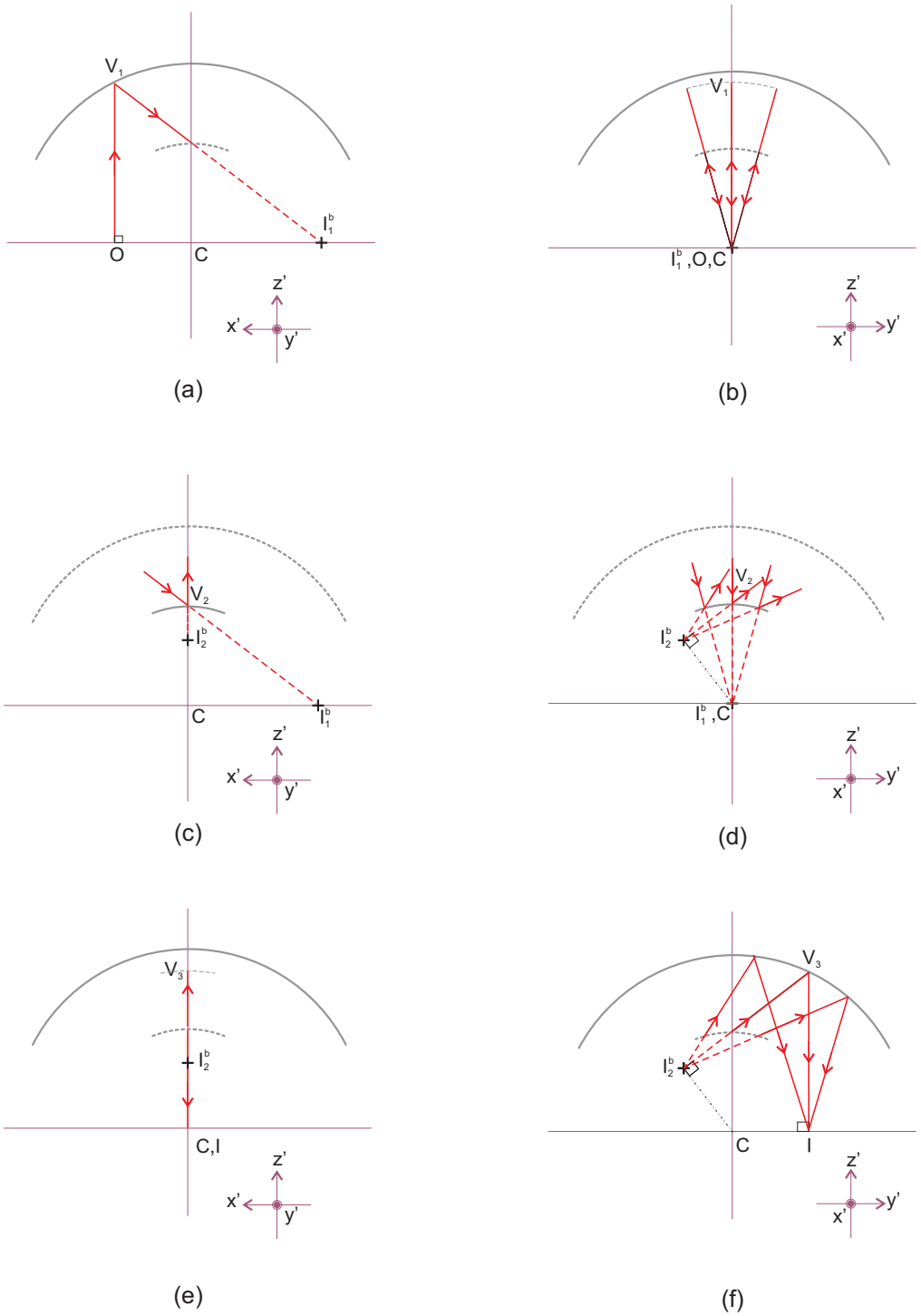


Fig. 6. Similar to Fig. 5 but showing the path followed by the bundle of rays departing from design point *O* on a plane parallel to the Y'Z' plane.

The final image, besides being anastigmatic, is also free of coma. This is due to the Rowland layout of the object point and the a-comatic property of the intermediate images

#126592 - $15.00 USD Received 6 Apr 2010; revised 14 May 2010; accepted 14 May 2010; published 28 May 2010

noted in previous section. Furthermore, the zero order image $O'$ is also anastigmatic and a-comatic, as with the Offner relay system. Therefore, there are two high quality image points on the spectral axis: the image at the quadrature wavelength $\lambda_q$ and the image at zero wavelength. The expected result is an acceptable image quality for intermediate wavelengths, that is, for wavelengths shorter than $\lambda_q$.

It is worth noting the tolerance of the Offner spectrometer in quadrature against small changes in the design parameters. For example, a reduction of the grating radius can be compensated by decreasing the angle $\theta_1$. This means that the design point approaches the curvature center, but its image at the design wavelength remains anastigmatic. Likewise, a change in the grating density only affects spectral dispersion. In both cases, the wavelength $\lambda_q$ verifying the quadrature condition is modified, but the image quality remains essentially unchanged.

To complete this section, a summary is given of the main formulas used to develop a spectrometer like the one discussed. The first formula relates the angle of incidence of the reference ray on the first reflection $\theta_1$ with the wavelength of design $\lambda_q$. It is obtained from Eq. (6) by taking $\alpha = \pi/4$ and $\theta = 2\theta_1$:

$$\sin(2\theta_1) = m\frac{\lambda_q}{\sqrt{2}d} \tag{7}$$

The second formula determines the object and image position as a function of $\theta_1$. It results from the Rowland and concentricity conditions:

$$CO = R_1 \sin\theta_1 = R_2 \sin(2\theta_1) = CI \tag{8}$$

The third formula refers to the spatial extent of the spectral image $h$ for a given spectral range $\Delta\lambda$:

$$h = \sqrt{2}CO\frac{\Delta\lambda}{\lambda_q} \tag{9}$$

This last equation is obtained under the hypothesis that the spectrum extends linearly along the line connecting image $I$ at diffraction order $m$ and the zero order image $O'$.

## 4. Design examples

In this section we present some examples of design of Offner spectrometers in the quadrature configuration based on the set-up discussed in the previous section. All examples correspond to simulations made using commercial optical design software OSLO [16]. Each example specifies the spectral band, the *f*-number and the image size. Free parameters in the simulations are the grating density ($1/d$), the point on the slit ($O$) and the wavelength ($\lambda_q$) that has its image in quadrature (the design object point and the design wavelength). For a given set of these parameters, the radius of the convex grating is calculated by combining Eqs. (7-9):

$$R_2 = \frac{hd}{\Delta\lambda} \tag{10}$$

where $m = 1$. Next, the angle of incidence of the reference ray on the concave mirror $\theta_1$ is determined by using Eq. (7) and the radius of the concave mirror is calculated from Eq. (8). This last equation also gives the position of the object $O$ and its image $I$. The image plane is taken as the plane containing $C$, $O$ and $I$.

#126592 - $15.00 USD Received 6 Apr 2010; revised 14 May 2010; accepted 14 May 2010; published 28 May 2010

In our design procedure, two of the three free parameters are set at the beginning of the simulation (typically, the design point and wavelength) and the other one is allowed to vary until the focal spots are optimized or vignetting occurs. We stress that vignetting is fully avoided in the examples presented below. Finally, a small tilt is applied to the image plane in order to reduce the size of focal spots even further.

Before presenting some specific examples, we shall comment on some general characteristics of the simulations. First, the design wavelength chosen is the larger one (or close to it), in contrast to in-plane spectrometers where design wavelength is near the spectrum center. This is done because shorter wavelengths approach the center of the system where the optical aberrations are smaller. Likewise, at first glance it might be preferable to choose the design point $O$ close to the slit far end. However, vignetting appears to be a limiting factor, so typically $O$ must be chosen nearest the inner border of the slit. Anyway, more compact designs are achieved providing $O$ approaches the slit center. Finally, the system is limited by the slit size. Although a very small geometrical image is attained for the design point, astigmatism increases dramatically for the images of points on the slit located farther away from the center of curvature. Moreover, if we try to increase the slit length toward the curvature center, vignetting appears at shorter wavelengths, as can be guessed from Fig. 1c. In contrast, the spectral axis is what limits the performance in the Offner in-plane systems.

**Table 1. Specifications and performance for the Offner imaging spectrometer in quadrature of example 1**

| Specifications | | Parameters of design | | Image quality [a] | |
|---|---|---|---|---|---|
| Spectral range (nm) | 400-1700 | Grating density (lines/mm) | 400 | RMS spot diameter (μm) | 21.15 |
| Reciprocal linear dispersion (nm/μm) | 0.087 | Grating radius (mm) | 28.85 | 80% ensquared energy (μm) | 24.75 |
| Object height (mm) | 6.5 | Mirror Radius (mm) | 55.89 | Smile (μm) | 0.8 |
| *f*-number | 4 | Image plane tilt (degrees) | −1.05 | Keystone (μm) | 0.11 |

[a] Worst values for full field and spectral range are shown

## Example 1

The first example corresponds to a broadband spectrometer with a spectral range from 0.4 to 1.7 μm. This system can be built with a beam-splitter and two array detectors in the image plane. For example, the first one can be a CCD camera for the 0.4-0.9 μm spectral band, and the second one, an InGaAs array detector for the 0.9-1.7 μm spectral band. The specifications for this spectrometer are shown in Table 1 (left columns). The center columns describe the design parameters for an optimized spectrometer in quadrature, and the right-hand ones give the image and distortion characteristics of the system. With regard to image distortions, smile describes the change of dispersion angle with field position and keystone refers to the change of magnification with wavelength. Both parameters are measured with respect to the centroid of the geometrical image. Even though our design is optimized only for small spot sizes, it also provides low spatial and spectral distortion (less than one percent of the spot size). This is very helpful in the processing of the spectroscopic information.

For comparison, we have simulated the performance of an in-plane Offner spectrometer with the same specifications and similar size but with two concave mirrors to compensate for the asymmetry on diffraction in the grating. The similar size has been achieved by choosing the same density of grating grooves as in the quadrature system. The in-plane spectrometer has been optimized following the procedure detailed in Ref. [9]. obtaining a worst spot size

#126592 - $15.00 USD Received 6 Apr 2010; revised 14 May 2010; accepted 14 May 2010; published 28 May 2010

over five times greater (about 100 μm RMS spot diameter); smile distortion is also five times greater, while keystone distortion is two orders of magnitude greater. To get a spot size similar to the one obtained with the off-plane configuration, the *f*-number has to be increased to 7.8. Another way to decrease the spot size in the in-plane configuration is to reduce the grating density at the expense of increasing the size of the spectrometer. In the quadrature configuration, the size of the system is so small (over a volume of 7 x 3 x 3 $cm^3$) that it can be made monolithic. This can be advantageous for increasing the aperture of the spectrometer. For example, if the spectrometer is built on glass with an average refractive index of 1.6, the *f*-number reduces to 2.5, a very acceptable value.

## Example 2

A second example corresponds to a spectrometer with a smaller bandwidth. Some possible applications are Raman spectroscopy or spectral characterization of ultrashort laser pulses. The example presented includes a spectral range from 765 to 985 nm suitable for analyzing the Raman spectrum provided with an excitation laser around 750 nm. Table 2 summarizes the specifications and results obtained from an optimized quadrature and an optimized in-plane configuration. In this example, the difference of spot size is smaller than in the previous example, but the image quality of the quadrature configuration is even better, while distortions are similar in both systems. Nevertheless, if a slightly worse spectral resolution is tolerable, the slit length can be increased to more than 17 mm in the in-plane configuration without changing the spot size significantly. This is because, in this configuration and range of slit lengths, the worst spot size is obtained at a point on the axis. A similar image quality is achieved in the off-plane configuration for smaller slit lengths of up to 15.8 mm.

**Table 2. Specifications and performance for the Offner imaging spectrometers in example 2**

| | Quadrature | | In-plane |
|---|---|---|---|
| Spectral range (nm) | | 765-985 | |
| Reciprocal linear dispersion (nm/μm) | | 0.022 | |
| Object height (mm) | | 10 | |
| *f*-number | | 3.4 | |
| Grating density (lines/mm) | | 600 | |
| Grating radius (mm) | 75.76 | | 75.76 |
| Mirror Radius (mm) | 148 | | 129.31, 146.13[a] |
| RMS spot diameter (μm) | 16.88 | | 45.32 |
| 80% squared energy (μm) | 21.47 | | 46.32 |
| Smile (μm) | 0.13 | | 0.46 |
| Keystone (μm) | 0.11 | | 0.06 |

[a] For an in-plane spectrometer with two concave mirrors

#126592 - $15.00 USD Received 6 Apr 2010; revised 14 May 2010; accepted 14 May 2010; published 28 May 2010

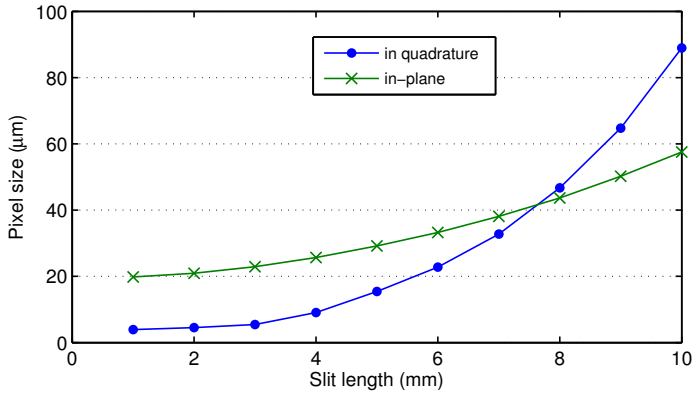


Fig. 7. Pixel size as a function of the slit length for the quadrature and in-plane spectrometers in example 3.

### Example 3

The third example is for a spectrometer in the VIS-NIR spectral band between 400 and 1000 nm, which matches the spectral range of a typical CCD camera. This spectral band has been set to spread over a 10 mm length and the *f*-number chosen was 4. In this case, the grating density is set so that the overall length of the system does not exceed 60 mm. This is verified for a grating density of 550 lines/mm and 530 lines/mm in the quadrature and in-plane configuration, respectively. Figure 7 shows the plot of the pixel size for both optimized systems as a function of the spatial image size (the object or slit length). To define the pixel size $p$ we use a square with side $p$ that contains 80% energy of any image point. For small slits, the quadrature configuration has a better image quality, but as the slit length increases, the spot size also increases considerably, so the in-plane system works better. The spatial performance of the system can be stated in relation to the number of spatial image points (slit length divided by pixel size). This provides better performance for the quadrature configuration and a 3 mm slit, obtaining over 550 spatial pixels. In a practical system, the spectrometer fore-optics (not discussed here) must be adapted to obtain a high quality image of the desired scene from this size slit.

### Example 4

As a final example, let us look at the spectrometer discussed in [14]. The off-plane configuration is very different, with the plane of incidence almost parallel to the grating grooves, as in Fig. 1b (using our notation $\alpha$ is nearly $\pi/2$). In this example, the spectral band of the spectrometer extends from 0.92 to 1.32 μm and spreads over a length of about 7.14 mm, the slit length is 6 mm, the radius of the concave mirror is set to 70 mm and the *f*-number to 4. In the design of ref [14], 77% of energy was contained in a square with an 18 μm side. With our configuration, we get 80% energy in a square of 12 μm side and 100% energy in a square of 16 μm side (see Fig. 8).

## 5. Summary and conclusions

We have presented a very simple design procedure that allows for the development of high quality Offner type spectrometers in a new arrangement: the quadrature configuration. This procedure is based on an analytical approach derived from the aberration theory of classical spherical diffraction gratings. Some illustrative examples show that these spectrometers allow

#126592 - $15.00 USD Received 6 Apr 2010; revised 14 May 2010; accepted 14 May 2010; published 28 May 2010

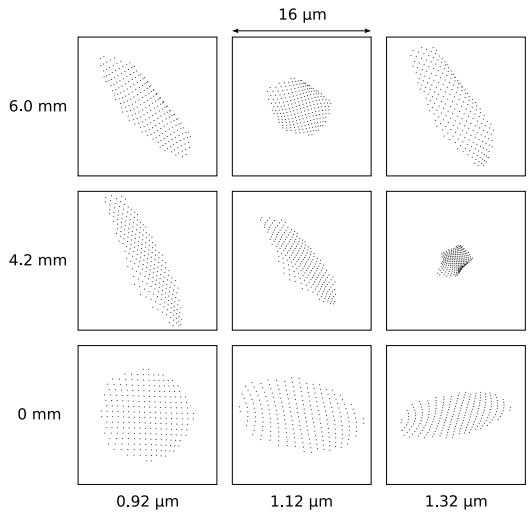


Fig. 8. Geometrical spots diagrams for the imaging spectrometer in example 4 for three object height (0, 4.2 and 6 mm) and three wavelengths, (0.92, 1.12 and 1.32 μm). The design point is at 3.6 mm and the design wavelength is 1.256 μm

for very compact design and high spectral resolution in different spectral bands ranging from a few hundred to more than one thousand nanometers in the VIS-NIR. One of the factors that limits the system performance is vignetting, which affects the slit length, especially for spectrum ranges greater than an octave. Slit length and spatial resolution are also limited by astigmatism, which increases considerably as the object point on the slit separates from the design point far away from the center of the system.

Even though in the examples presented, the performance of the quadrature configuration is greater than that of a similar in-plane configuration, it does not mean that the quadrature arrangement is always superior. If we allow for larger system dimensions and require high spatial resolutions, the in-plane system must be the spectrometer of choice. Besides this, for a given image size, vignetting restricts the system size in the quadrature arrangement. Accordingly, larger systems must have large *f*-numbers. On the contrary, compact systems can be built monolithically allowing for a high luminous flux.

We have restricted our analysis to the symmetric quadrature configuration ($\alpha = \pi/4$) where the angle of diffraction of the reference ray for the design wavelength matches the angle of incidence on the grating. The same analytical procedure with few changes can also be applied to the design of asymmetric quadrature configurations ($\alpha \neq \pi/4$). However, they require the concave mirror to be split into two reflectors with different radii to achieve a similar performance. Other off-plane configurations (out of quadrature), such as the one discussed in [14], are also feasible but, unfortunately, the analytical theory needed to develop anastigmatic off-plane, "off-quadrature" systems is certainly more complicated than the one presented here. In spite of this, the properties of these and other designs can be estimated quickly by using fast computational tools easily available nowadays. We expect that this work will encourage other researchers to look for new designs beyond in-plane geometries, both analytically and numerically, in the same way that the work in refs [13]. and [14] has stimulated us.

**Acknowledgments**

The authors hereby express their acknowledgment to the Xunta de Galicia for providing financial support (contract 07MDS035166PR).

#126592 - $15.00 USD Received 6 Apr 2010; revised 14 May 2010; accepted 14 May 2010; published 28 May 2010